Research Article

Dominik Kukla*, Mateusz Kopec and Andrzej Gradzik

Identification and characterization of the grinding burns by eddy current method

https://doi.org/10.1515/eng-2022-0382
received August 12, 2022; accepted October 26, 2022

Abstract: This work presents an attempt to identify local changes in materials caused by local grinding burnings by using the eddy current (EC) method. The locally heat-treated AISI 9310 steel specimen was prepared by using a laser surfacing process to imitate three different grinding burns. These burn marks were characterized in terms of changes in microstructure and hardness on the surface and cross-section of the specimen. On such a basis, the depth of the heat-affected zone caused by the grinding tool was examined. Subsequently, the specimen was subjected to the EC measurements for the quantitative description of the signal from each of the defects by using a commercial NORTEC 600D flaw detector working in specimen scanning mode and with a pencil probe. The changes in the amplitude and the phase angle of the signal from three defects indicate the possibility to identify burns along with their quantitative description and subsequent estimation of their depth. The differences in the phase angle value, related to the local changes in the stress state, serve as an effective indicator of the specimen overheating degree in the area of the EC induction.

Keywords: eddy current, non-destructive testing, hardness, heat-treatment

1 Introduction

Grinding burns are one of the critical issues affecting components' surface integrity and frequently leading to their failure. The majority of existing methods for grinding thermal damage identification are based on offline characteristics, for example, residual stress and microhardness measurements, or visual methods for burned color identification [1]. In recent years, the development of non-destructive techniques for grinding burns detection based on X-ray diffraction [2], acoustic emission [3], and magnetic methods [4] was observed. Magnetic methods such as Barkhausen noise [5] or eddy current (EC) method are nowadays frequently applied for the detection of burns without the subjectivity of the inspector (acid etching method). However, the potential application of these methods during in-process inspection has not been investigated in detail as yet [6]. The EC method is a conventional and effective technique used in defectoscopy. This technique could be used in discontinuity detection as well as for the localization of recognized changes in microstructure and properties generated at the manufacturing, heat treatment, or exploitation stage [7]. It was found that one of the potential EC applications could be the detection of grinding burns resulting from local overheating of the material due to the improper surface treatment performed. As-formed grinding burns occur during heat treatment of hardened elements, including grinding wheels, and frequently cause increased degradation of the workpieces which leads to subsequent component failure. For such reason, it is important to develop diagnostic methods for the detection of manufacturing defects, preferably with the support of non-destructive techniques. The subject of the research was therefore to examine the possibility of the EC technique and the commercial flaw detector application in the identification and assessment of locally overheated areas resulting from the laser processing that was previously used to simulate grinding burns.

* **Corresponding author: Dominik Kukla,** Department of Experimental Mechanics, Institute of Fundamental Technological Research Polish Academy of Sciences, Warsaw, Poland, e-mail: dkukla@ippt.pan.pl
Mateusz Kopec: Department of Experimental Mechanics, Institute of Fundamental Technological Research Polish Academy of Sciences, Warsaw, Poland, e-mail: mkopec@ippt.pan.pl
Andrzej Gradzik: Department of Mechanical Engineering and Aeronautics, University of Technology in Rzeszow, Rzeszów, Poland, e-mail: andrzej_gradzik@prz.edu.pl

2 Methodology

In a standard EC test, a circular coil carrying current is located in the proximity of the electrically conductive test specimen. An alternating current in the coil generates a changing magnetic field, which interacts with the test

Table 1: Chemical composition of AISI 9310 steel

C	Ni	Cr	Mo	Cu	Mn	Si	P	Fe
0.13	3.18	1.21	0.11	0.07	0.57	0.28	0.008	Bal.

specimen and subsequently generates ECs. Variations in the phase and magnitude of these ECs can be monitored by using a second "receiver" coil, or by measuring changes in the current flowing in the primary "excitation" coil. The presence of metallurgical changes in the material, including burns, will cause a change in EC and a corresponding change in the registered signal. The main advantage of this method is that the inspection could be performed without contact and with some distance or lift off between the sensor and the part [8,9].

AISI 9310 steel (in accordance with the AMS 6265 standard) used in this study is a conventional material for aircraft gear production [10]. It is commonly subjected to thermo-chemical and mechanical surface treatment due to the strength and dimensional requirements for these elements. The chemical composition of the material is listed in Table 1.

The specimen with artificial defects produced with laser technique (Trumpf TruLaser Cell 3008) on the AISI 9310 steel was used to represent the burns during grinding (Figure 1a). Microstructural observations were performed on the etched specimens using a Nikon Epiphot 200 light microscope. Microhardness profiles were made under a load of 500 g by using the NEXUS 4303 hardness tester to estimate the depth of the heat-affected zone (HAZ) measured from the surface. The processing parameters and the values of the depth of burns and HAZ measured on the specimens' cross-section are presented in Table 2. The precise control of the power, speed, and power density of the laser beam enabled to obtain three different grinding burns (Figure 1b). These burns were characterized in terms of changes in the microstructure and hardness of their cross-sections. As-prepared specimens were subsequently subjected to the EC measurements for the qualitative description of each defect. This non-destructive testing was performed using the commercial flow detector Nortec 600D working in specimen scanning mode and with a pencil probe.

Figure 1 shows a general view of the specimen with three laser burns and a cross-sectional view of this specimen, revealing the microstructure and HAZs. EC testing was performed on the specimens before cutting and in perpendicular to the burns' axis direction. The pencil probe and four frequencies of induction current were used to achieve different depths of material penetration. For each linear scan, the signal parameters in the form of amplitude and impedance phase angle were recorded.

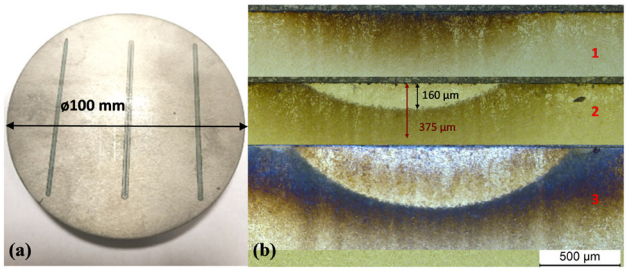

Figure 1: General view of the specimen with linear burns: (a) cross-sectional view of the burns in specimen and (b) 1, 2, and 3 are the burn number.

3 Result

The representative result of EC testing obtained for the frequency of 500 kHz was presented in the form of indications on the defectoscope screen as shown in Figure 2a. Additionally, Figure 2b and c present the results of amplitude and phase angle measurements performed in the range of frequency from 500 kHz to 6 MHz, respectively. Slight differences in the values of both parameters depending on the measuring frequency were attributed to the high magnetic permeability of the hardened layer, which limits the penetration of ECs to a depth of several hundred micrometers into the material [11].

Table 2: Laser processing parameters and depth of burns and HAZ measured on the cross-sections

Burn number	Power of the beam (W)	Speed of the beam (mm/min)	Power density (W/cm^2)	Depth of the burn (µm)	Depth of the HAZ (µm)
1	80	250	2,550	150	220
2	140	750	4,450	160	375
3	160	500	5,100	425	550

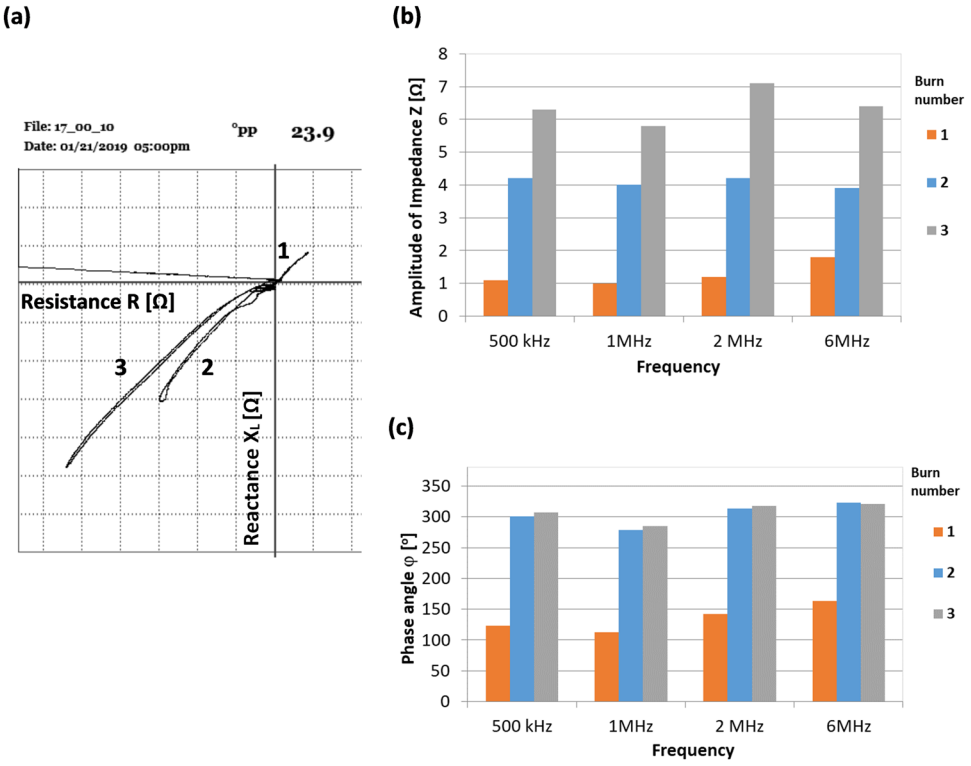

Figure 2: View of the defectoscope screen with three burn indications (a). The measurement results of the impedance amplitude (b) and phase angle (c) for four measuring frequencies.

Based on the cross-sectional observations, a qualitative assessment of the depth of burns and HAZs was conducted (Figure 3). Furthermore, hardness profiles were performed along the axis of each of the burns to measure the hardness distribution from the surface to the core (Figure 4). The microstructural observations and the hardness profiles were subsequently correlated with the measured values of the impedance and phase angle as shown in Figures 3 and 5, respectively. The comparison of values obtained from the EC method and the depth of burns and HAZ is almost in perfect agreement. In defectoscopy, the amplitude of the impedance signal depends on the change in the depth of the defect in relation to the reference value. Similarly, the changes in impedance during the scanning of various depths of burns could be explained. If the depth of the anomalous area increases, the difference in the impedance value and the reference value is higher as well. Such preliminary analysis shows the potential of non-destructive assessment in structure defect depth estimation during EC measurements of impedance amplitude (Figure 3).

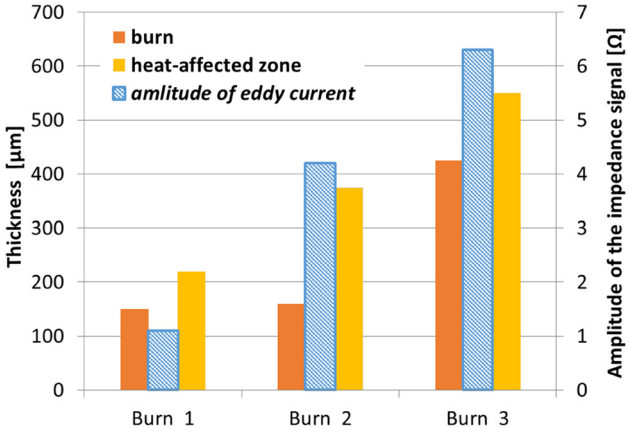

Figure 3: The burn and HAZ thickness dependence on impedance signal amplitude.

On the other hand, the relation between the hardness in the overheating areas and the value of the impedance phase angle was assessed. As could be seen in Figure 4, the microhardness profiles performed on the cross-sections of the three different types of burns were different. The differences found in profile no. 1 were caused by the specific parameters of the laser treatment and subsequent changes in the specimen microstructure related to the level of the residual stress on the workpiece surface being altered in the grinding process by the action of applied mechanical forces, thermal stress, and stress owing to phase transformations [12,13]. These changes were related,

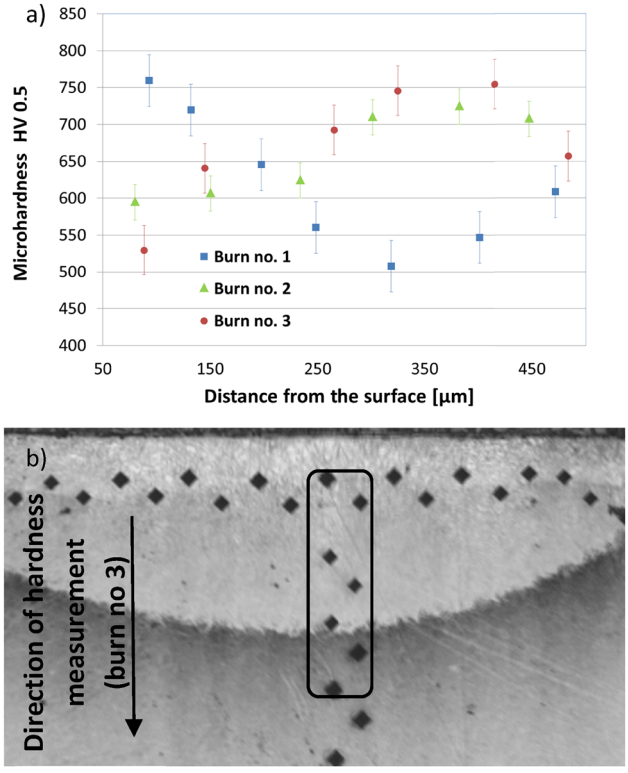

Figure 4: Microhardness distribution on the cross-sections with a gradient of hardness caused by laser heating (a) and microscopic view of the investigated area (b).

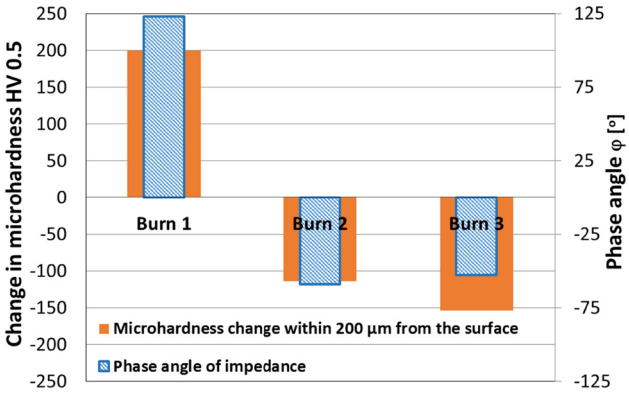

Figure 5: Comparison of results of changes in the microhardness at a distance of 200 µm from the surface and values of impedance phase angle measured for each burn.

among others, to the creation of excessive tempering zones and re-quenching, resulting in significant properties in the layer of the processed material. The comparison of the microhardness results with the values of the phase angle measured during linear scanning presents a strong correlation between these parameters. The microhardness at the burn point, as a function of the distance from the surface, changes in the same way as the impedance trajectory in these areas, which could be observed in Figure 2a. The summary of the work's findings is presented in Figure 5 to further confirm this correlation.

One could observe the dependence of the parameters induced in the material due to EC measurement on its surface hardness. Changes in the structure and stress state of ferromagnetic materials caused by grinding burn increase the magnetic permeability in the metamorphic layer [12]. Since such an increase is proportional to the hardness changes related to the burn and the permeability affects the value of the EC phase angle [14], it could be deduced that its changes enable a qualitative assessment of changes in hardness at a specific distance limited by EC depth penetration [15,16].

The presented result extends the potential application of EC measurements to the assessment of the surface and sub-surface hardness changes through variation in the value of the impedance phase angle. Although such an assessment is qualitative, it still enables a non-destructive detection of hardness changes related to grinding burns.

4 Conclusion

The EC technique enables the qualitative identification of local hardness changes caused by excessive grinding. One can find that with an appropriate set of reference specimens with defined depth and surface hardness, it is possible to quantify the burns, based on the analysis of changes in the phase angle and the amplitude of the signal obtained during scanning of the machined surface.

Conflict of interest: Authors state no conflict of interest.

References

[1] Szczepankowski A, Przysowa R, Perczyński J, Kułaszka A. Health and durability of protective and thermal barrier coatings monitored in service by visual inspection. Coatings. 2022;12(5):624. doi: 10.3390/coatings12050624.

[2] He B, Wei C, Ding S, Shi Z. A survey of methods for detecting metallic grinding burn. Measurement. 2019;134:426–39. doi: 10.1016/j.measurement.2018.10.093. ISSN 0263-2241.

[3] Eda H, Kishi K, Usiu N, Kakino Y, Fujiwara A. In-process detection of grinding burn by means of utilizing acoustic emission. J Jpn Soc Precis Eng. 1983;49(9):1257–62. doi: 10.2493/jjspe1933.49.1257.

[4] Santa-aho S, Vippola M, Sorsa A, Latokartano J, Lindgren M, Leiviskä K, et al. Development of Barkhausen noise calibration

blocks for reliable grinding burn detection. J Mater Process Technol. 2012;212:408–16.
[5] Neslušan M, Cížek J, Kolarˇík K, Minárik P, Čilliková M, Melikhova O. Monitoring of grinding burn via Barkhausen noise emission in case-hardened steel in large-bearing production. J Mater Process Technol. 2017;240:104–17.
[6] Khazi I, Kovacs A, Mescheder U, Zahedi A, Azarhoushang B. Fusion of optical and microfabricated eddy current sensors for the non-destructive detection of grinding burn. Adv Sci Technol Eng Syst J. 2021;6(1):1414–21.
[7] Lanzagorta JL, Urgoiti L, Vazquez PR, Barrenetxea D, Sánchez JA. Experimental approach for a grinding burn in-process inspection system based on eddy current. Procedia CIRP. 2020;87:391–6. doi: 10.1016/j.procir.2020.02.011.Mook.
[8] Ito R, Mukaide N, Azuma T, Soma S, Murakami S, Kuriyagawa T. Development of non-destructive inspection system for grinding burn-in-process detection of grinding burn. Adv Mater Res. 2014;1017:135–40.
[9] Wasif R, Tokhi MO, Shirkoohi G, Marks R, Rudlin J. Development of permanently installed magnetic eddy current sensor for corrosion monitoring of ferromagnetic pipelines. Appl Sci. 2022;12(3):1037. doi: 10.3390/app12031037.
[10] Krantz T, Tufts B. Pitting and bending fatigue evaluations of a new case-carburized gear steel. Gear Technol. 2008;2:52–63.
[11] He B, Wei C, Ding S, Shi Z. A survey of methods for detecting metallic grinding burn. Measurement. 2019;134:426–39. doi: 10.1016/j.measurement.2018.10.093. Elsevier B.V.
[12] Ma X, Peyton AJ, Zhao YY. Eddy current measurements of electrical conductivity and magnetic permeability of porous metals. NDT E Int. 2006;39(7):562–8. doi: 10.1016/j.ndteint.2006.03.008.
[13] Dychtoń K, Gradzik A, Kolek, Raga K. Evaluation of thermal damage impact on microstructure and properties of carburized AISI 9310 gear steel grade by destructive and non-destructive testing methods. Materials (Basel). 2021;14(18):5276. doi: 10.3390/ma14185276.
[14] Akujärvi V, Cedell T, Gutnichenko O, Jaskari M, Andersson M. Evolution of magnetic properties during tempering. Int J Adv Manuf Technol. 2022;119(3–4):2329–39. doi: 10.1007/s00170-021-08464-7.
[15] Chen B, Ren S. Study on the relationship between permeability, hardness of ferromagnetic structure and quenching, tempering temperature. Proceedings of 2021 IEEE Far East NDT New Technology and Application Forum, FENDT 2021; 2021. p. 16–21. doi: 10.1109/FENDT54151.2021.9749635
[16] Zösch A, Seidel C, Härtel K, Seidel MW, Maier J, Neun G. Detection of near Surface damages in crank shafts by using eddy current testing. 19th World Conference on Non-Destructie Testing; 2016. p. 8.